



August 22th-25th, 2017

Pernambuco, Brazil



Gradient based Investigation over Northeast Brazil and its conjugate West African Margin

Maurya, V. P.¹; Fontes, S. L.²; La Terra, E. M. F.³

Postdoctoral Researcher at COGE – ON¹; Senior Researcher at COGE– ON²; Researcher at COGE– ON³
ved.maurya@on.br¹; sergio@on.br²; laterra@on.br³.

Introduction

Cross-gradient method may provide the geomorphological correlation among individual images (Gallardo and Meju 2004). A joint application of gradient properties for different geophysical fields can emphasize individual regional trends with different levels and types of correlations. Jilinski et al. (2013) used the angular difference between gradient directions of potential field and bathymetry, to correlate them in order to provide tentative COB location.

The available marine gravity (Sandwell et al., 2014) and magnetic (Maus et al., 2009) grids from satellite over South and mid-Atlantic oceans are shown in Fig. 1. Marine gravity reveals edge of the continental shelf with a continuous, prominent and elongated gravity high, trending subparallel to the coastal regions (Fig. 1A). The “edge effect” gravity high is mostly observed at passive continental margins (Rabinowitz and LaBrecque, 1979). The possible explanation for the “edge effect” are related to the depth of major lateral, near-seafloor density variation, the equivalent base crust compensation depth (Talwani and Eldholm, 1972), the juxtaposition of continental and oceanic crust (Rabinowitz and LaBrecque, 1979), and magmatic underplating (Watts, 2001). Generally, magnetization of oceanic and continental crust differs significantly. The cooling age of seafloor and linked isochrons of magnetic anomalies widely used to determine COB and reveals history of seafloor spreading. Magnetic data gives reliable source of information to identify the oceanic crust with the appearance of spreading-related linear magnetic anomalies. However, observed magnetic anomalies for study area are still sparse enough to map distinct magnetic lineaments (Hemant and Maus, 2005). Thus, spread related linear magnetic anomalies are very weak for the study area compared to other parts of south and mid-Atlantic oceans (Fig. 1B).

We investigated conjugate margins of Northeast Brazil and West Africa (study area is shown in Fig. 1 by dashed rectangles) using gradient-based correlation approach i.e., TTAC method, applied over gravity and magnetic anomalies of potential field data. Previously, we used the TTAC approach only for gravity data (Maurya et al. 2017a & b). However, this approach may suit for the magnetic anomalies too. This time, we utilize the TTAC approach both for gravity and magnetic anomalies individually as

both represent distinctive character along the continental passive margins. However, joint correlation between both methods provides erroneous results related to differences in resolution of available global magnetic and gravity grids i.e., magnetic grid resolution is almost two times lower than the gravity grid.

Methodology

First, Bouguer gravity (shown in Fig. 2A) was estimated for the study area from the high-resolution radar altimetry derived satellite gravity data of ~ 1 min resolution (Sandwell et al., 2014) and SRTM topography grid of ~ 30 arc-sec resolution. Deduced Bouguer gravity corrected for Bouguer slab, curvature and terrain corrections with FA2BOUG code (Fullea et al. 2008). For terrain corrections in rugged topography areas, we used high-resolution SRTM topography grid with ~ 15” resolution. Reduction densities for crust and seawater considered as 2670 and 1030 kg/m³, respectively. Bouguer gravity maps lows over the continental and highs with oceanic domains (Fig. 2A). Moreover, magnetic spread related linear magnetic anomalies are weak for the study area, thus, cannot provide the distinction between oceanic and continental crust (Fig. 2B). We applied TTAC approach (more detailed methodology description in Maurya et al. 2017a & b) using tilt and theta derivative based filters, for gravity data. TTAC approach gives the correlation between geomorphological features of different crustal types (Maurya et al. 2017a & b). We also applied TTAC approach for the magnetic anomaly of the study area to distinguish crustal types likewise gravity.

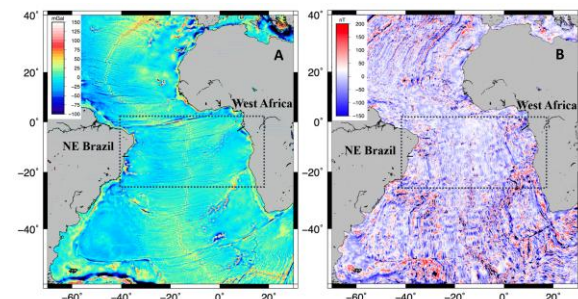


Figure 1: Satellite (A) gravity (Sandwell et al., 2014) and (B) magnetic (Maus et al., 2009) anomalies. Dashed lines show the rectangle covering only the study area.

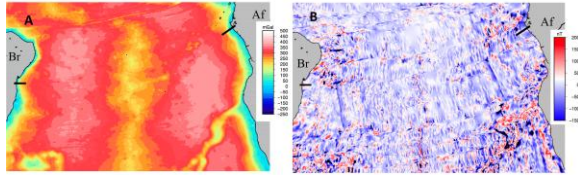


Figure 2: Bouguer Gravity (A) and Magnetic anomalies (B) map of the study area. Location of the study area is shown in Fig. 1 with dashed rectangle.

Results and Discussion

We computed tilt and theta over the study area both for gravity and for magnetic data (Figures 3 & 4). Theta map for gravity data delineates the edges associated with regional as well local geological boundaries. Over edges, theta depicts very small values of ~ 0 (Fig. 3A). Theta map for magnetic data picks some edges associated with volcanic rich margins (Fig. 3B). Moreover, linear magnetic anomalies linked with sea-floor spreading is almost absent over the study area for both of the conjugate margins.

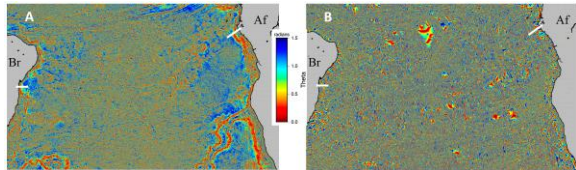


Figure 3: Theta map for gravity (A) and magnetic (B) data for the study area.

Tilt map for gravity data (Fig. 4A) distinguishes the crustal types as negative tilt represents continental crust with low-density sources, positive tilt depicts oceanic crust linked with high-density sources and zero tilt values marks the boundaries and or edges. Tilt map for magnetic data possibly highlights spreading related linear anomalies as compared to theta map (Fig. 4B) with limited resolution. Moreover, positive tilt long wavelength feature associated highs mostly observed over the transition crust.

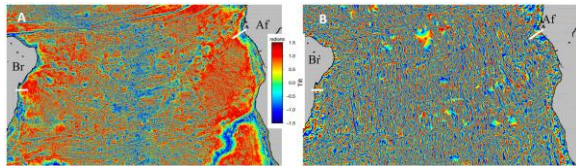


Figure 4: Tilt map for gravity (A) and magnetic (B) data for the study area

We applied TTAC approach first over gravity data (Fig. 5A) and then over the magnetic data (Fig. 5B). TTAC application over gravity data finds the major crustal types, lineaments, fracture zones and oceanic ridges and or rises. In general, continental crust depicts inverse correlation, and oceanic crust depicts direct correlation. Thus, change in correlation marks the possible COB for the conjugate margins of study area. Nevertheless, Walvis ridge and Rio Grande rise depicts inverse correlation very similar to oceanic crust (Fig. 5A). TTAC of magnetic data shows reversal in correlation signature as continent depicts mostly direct correlation and beginning of oceanic crust depicts mostly inverse correlation (Fig. 5B). COB is marked by change in correlation from direct to inverse for magnetic data, which is opposite to gravity data. Alternating positive and negative linear correlation anomalies are also observed over oceanic region.

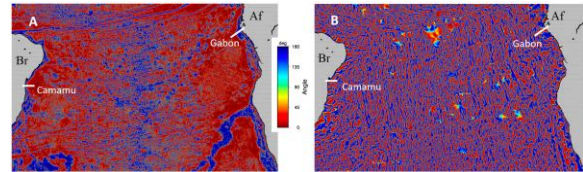


Figure 5: TTAC map for gravity (A) and magnetic (B) data for the study area.

Finally, we validated the TTAC application for both gravity (Fig. 6) and magnetic data (Fig. 7) for the study area with Camamu-Gabon margin transects. To test our COB estimation (marking the change in correlation from inverse to direct), we extracted the tilt, theta and TTAC filter for gravity data along the conjugate marginal transects of Camamu and Gabon basins. Blaich et al. (2011) provided a combined interpretation of gravity, magnetic and seismic data along both the conjugate margin transects (shown by green vertical lines). We also included the recent interpretation from Heine et al. (2013) from plate reconstruction studies along the same marginal transects.

TTAC for gravity data over Camamu does not give reasonable COB location as compared to other approaches. A possible explanation is the presence of extreme shallow Moho reflector for the transitional crust from the available seismic lines, which hinders the possible COB demarcation in gravity data. TTAC for Gabon transect provides the COB at the same location as Blaich et al. (2011) interpretation. LaLOC and Blaich's COB shows minor discrepancy.



August 22th-25th, 2017

Pernambuco, Brazil

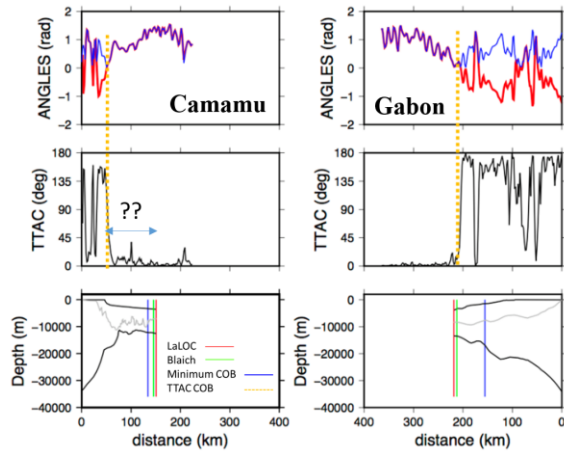


Figure 6: TTAC approach applied over gravity data for Camamu-Gabon conjugate margin transect. Marginal cross-sections along the marginal transects taken from Blaich et al. (2011) includes seabed (top), basement (middle) and Moho (bottom) variation. LaLOC (red line) and min COB (blue line) estimation is from Heine et al. (2013). Yellow vertical dashed line is COB from TTAC.

TTAC application for magnetic data over Camamu provides COB location (change in correlation from direct to inverse opposite to gravity data) same as Blaich's interpretation. However, conjugate Gabon basin COB estimation depicts a deviation from Blaich's interpretation for the magnetic data unlike gravity. This possibly attributed to less resolution (~ 2 min) of magnetic data. Moreover, linear alternating direct and inverse correlation anomalies for the Gabon basin over ocean possibly related to the sea floor spreading related linear magnetic anomalies.

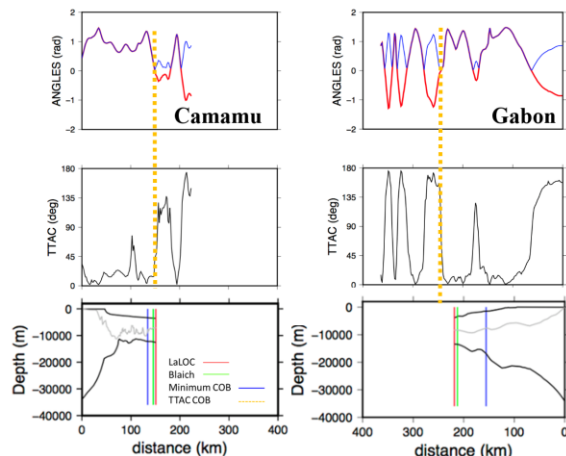


Figure 7: TTAC approach applied over magnetic data for Camamu-Gabon conjugate margin transects. Cross-sections description is similar as in Fig. 6.

Conclusions

TTAC application of both gravity and magnetic data gives the Continental-Oceanic Boundaries [COBs] estimates with good precision over both conjugate margin regions, and are consistent with previous results. Magnetic data were unable to distinguish crustal types, possibly due to lower resolution and very distinct magnetic source signatures in comparison to gravity anomalies. TTAC application over magnetic data delineates the possible magnetic intrusions as well spreading-related linear anomalies, mostly absent or weak in the map of magnetic anomalies. The conjugate margin Camamu-Gabon transects orthogonal to the extensional rift axis provides the reasonable COB interpretation for both gravity and magnetic data. COB deduced from correlation angles over northeastern Brazil is mostly uniform and consistent except Camamu basin, whereas, COB over Gabon basin is relatively wide compared to its conjugate Camamu basin. Moreover, transitional crust over Camamu basin has distinct M-reflector below rifted extensional margin from available seismic lines, representative of extremely shallow Moho discontinuity, which hinders its possible demarcation in gravity data. However, COB estimated from magnetic data using TTAC approach gives similar results as like previous interpretation. COB estimates for Gabon margin exactly matches with recent COB estimation from plate reconstruction studies for the gravity data but deviates for magnetic data, attributed to less resolution of magnetic data.

References

- Becker, J. J., D. T. Sandwell, W. H. F. Smith, J. Braud, B. Binder, J. Depner, D. Fabre, J. Factor, S. Ingalls, S-H. Kim, R. Ladner, K. Marks, S. Nelson, A. Pharaoh, G. Sharman, R. Trimmer, J. VonRosenburg, G. Wallace, P. Weatherall, 2009. Global Bathymetry and Elevation Data at 30 Arc Seconds Resolution: SRTM30_PLUS, Marine Geodesy, 32:4, 355-371.
- Blaich, O. A. Faleide, J. I. & Tsikalas, F. 2011. Crustal breakup and continent-ocean transition at South Atlantic conjugate margins, Journal of Geophysical Research, 116, B01402, doi: 10.1029/2010JB007686, 2011.
- Fullea J., Fernandez, M. & Zeyen, H. 2008. FA2BOUG - A FORTRAN 90 code to compute Bouguer gravity anomalies from gridded free-air anomalies: Application to the Atlantic-Mediterranean transition zone, Computers & Geosciences 34 (12), 1665-1681.
- Gallardo, L.A. & Meju, M.A., 2004. Joint two-dimensional dc resistivity and seismic traveltime inversion with cross-



August 22th-25th, 2017

Pernambuco, Brazil



gradients constraints, *J. Geophys. Res.*, 109, B03311, doi:10.1029/2003JB002716.

Hemant, K., & Maus, S., 2005. Geological modeling of the new CHAMP magnetic anomaly maps using a geographical information system technique, *J. Geophys. Res.*, 110, B12103, doi:10.1029/2005JB003837.

Jilinski, P., Meju Max A., and Fontes, Sergio L., 2013, Demarcation of continental-oceanic transition zone using angular differences between gradients of geophysical fields, *Geophysical Journal International*, 195(1), P.276-281.

Maurya, V.P., Fontes, S.L., La Terra, E.F., 2017a. An enhanced and effective technique for demarcation of continental – oceanic transition: application for South Atlantic Conjugate Margins, 79th EAGE Conference & Exhibition 2017 Paris, France.

Maurya, V.P., Fontes, S.L., La Terra, E.F., 2017b. A fast novel approach to locate continent-oceanic boundary over South American passive margin, 15th International Congress of the Brazilian Geophysical Society, Rio de Janeiro, Brazil, 31 July to 3 August.

Rabinowitz PD, LaBrecque J., 1979. The Mesozoic South Atlantic Ocean and evolution of its continental margins. *J Geophys Res* 84:5973-6002.

Sandwell, D.T., Muller, R.D. & Smith, W.H.F., 2014. New global marine gravity model from CryoSat-2 and Jason-1 reveals buried tectonic structure, *Science* 346, 65; DOI: 10.1126/science.1258213.

Watts, A.B., 2001. *Isostasy and Flexure of the Lithosphere*, Cambridge University Press, New York, 458 pp.



Genetic Comparison of Crude Oils from West Africa and South American Conjugate Basins

Craig Schiefelbein (1), William Dickson (2), Carlos Urien (3), John Zumberge (4)

(1) Geochemical Solutions International (craigs@geochemsol.com), (2) Dickson International Geosciences, (3) Urien & Associates, (4) Geomark Research

Introduction

Continuing research has clarified the tectono-structural history of the Atlantic conjugate margins. This includes the creation and segmentation of source rock depocenters. Petroleum geochemists have concurrently examined the nature and distribution of these associated source rocks by characterizing crude oils within a field, then a basin and across a series of basins. Crude oils possess important biological clues that can be used to unravel their genetic history from source to trap and beyond. Lacustrine source distributions of the South Atlantic were investigated by Brice et al., 1980; then comparisons of oil chemistries from both margins were published by Schiefelbein et al. (1997; 1999; and 2001).

Approach

Key geochemical indicators of source-rock paleoenvironments and age in the South Atlantic Margin (Mello, et al., 1988; Schiefelbein et al., 1999; Schiefelbein et al., 2001) have developed along with increasing numbers of samples and a broadening range of data (ie, deuterium isotopes, diamondoids) extracted from each sample. Our multi-parameter approach relied on a combination of parameters corresponding to the 'black oil' (>C15) component that are primarily influenced by source, but can also be affected by maturity and/or other alteration processes such as bio-degradation. Genetic relationships are established based on compositional similarity.

Multivariate statistical analyses [principal component analysis (PCA) and cluster analysis; Pirouette™, Infometrix, Seattle, WA.] are used to more clearly distinguish the different types of oils present throughout the South Atlantic Margin. Briefly, in PCA new independent variables are created (i.e., principal components) that are linear combinations of the original variables (i.e., geochemical parameters). The primary objective of PCA is to reduce the dimensionality of the data to a few important components that best explain the variation in the data. Prior to PCA, the original geochemical variables are auto-scaled (the mean value for each variable is subtracted and divided by the standard deviation) so that stable carbon isotope values (e.g., -30 ‰) can be meaningfully compared to sterane/hopane ratios, for example. The geochemical variables responsible for the PC axes can be viewed as a Loadings plot and the oil samples can be plotted in principal component space, PC1 versus PC2, as a Scores plot.

Hierarchical Cluster analysis (HCA) is an ancillary technique to PCA whereby a distance matrix is created from the scaled data; the distance between any two samples is a measure of their similarity (this distance is similar to a linear correlation coefficient; perfect correlation would have a value of 1.0 while poor correlation would have values < 0.5). The dendrogram is the output of a cluster analysis and shows groupings or clusters of oils.

Input variables are primarily source dependent and based on information obtained from the detailed analysis of the C15+ saturate and aromatic hydrocarbon fractions ('black oil'). The sixteen (16) source dependent variables used in the multivariate statistical analyses describe 68% of the variance and include the pristane/phytane ratio, the stable carbon isotopic compositions of the C15+ saturate and aromatic hydrocarbon fractions, and thirteen biomarker ratios, including the distribution of the 14 β , 17 β -C27, -C28 and -C29 steranes (from m/z 218), C27 Ts/Tm hopanes, C31-35 hopanes/C30 hopane, gammacerane/C30-hopane, C29-demethylated norhopane/C30-hopane, oleanane/C30-hopane and total steranes/total hopanes. Ratios based on the distribution of tricyclic and tetracyclic terpanes were also used: C21-Tri/C23-Tri, C26-Tri/C25-Tri, C24-Tetra/C26-Tri and the C30-Tetra/C27 diasteranes index (m/z 259).

Geochemical Data

Geochemical data utilized in this study are entirely non-exclusive and provided by Geochemical Solutions International, TDI Brooks International, Core Laboratories and/or Geomark Research. Sample locations in Figure 1.

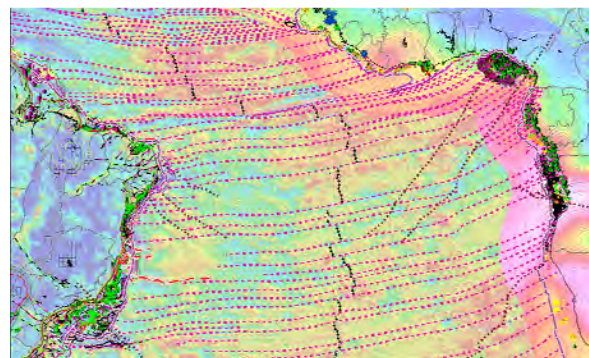


Figure 1: Distribution of crude oil, piston core, and source rock samples plus heat flow locations. The data set includes information from more than 1600 crude oils, 30,000+ source rocks from 220+ wells, 4000+ piston cores and 500+ heat flow measurements. (Gravity image compliments of GrizGeo)



Discussion

Our interpretive work began with the assembly of a data set and development of data intimacy through detailed inspection (e.g., see Dickson et al., 2016). Values from different laboratories that employed different analytical schemes required a determination of which measurements were common to all samples (the Lowest Common Denominator). Missing parameters from specific samples were supplied from analogues, sample averaging and standard relationships from other geochemical parameters based on physical proximity of sample sites and author experience. First-pass cross-plotting of key oil constituents and ratios showed main "anchor" clusters within a broad scatter of points on two- and three-axis plots. Outliers were then examined for causes of scatter, typically unique chemistries (e.g., Paleozoic source) or oils that experienced advanced maturity or extensive bio-degradation, resulting in compromised biomarker distributions.

Recognition and characterization of compositionally distinct oil types or families infers paleo-environmental conditions of source rock deposition and possible age. Clearest results are obtained from pure end-member oils from a single lithology, single paleo-environment source but this is uncommon to the South Atlantic margin with its compound basins, usually with drift-age marine fans overlying multi-stage rifts. Depositional environments may grade episodically from lacustrine to marine so that in late rift to sag phases, source rocks composed of mixed kerogens are deposited. Oils from such sources in similar phases of maturity may mimic mixed oils from discrete sources co-mingled in a common reservoir.

Results: Statistical Analyses

Statistical analysis of some 1500 oils allows separation into five major families: Early SynRift; Late SynRift/Sag; Marine/Mixed; Marine; Tertiary Deltaic (Figures 2 and 3). Incorporation of additional geologic constraints from tectono-structural mapping suggest that oil family and sub-family distributions (Figure 4) often relate to sediment thickness and basin to sub-basin structure; lacustrine oils show strong correlations of age and location between conjugate salt basins; and marine oils demonstrate age correlations related to global ocean anoxic events.

Source paleoenvironment and age are inferred, often using key biomarkers such as n-propyl C₃₀ steranes that only have marine precursors (Moldowan, et al., 1990) or oleanane, a specific biomarker associated with higher land plants and, in this study, a Tertiary source (Moldowan, et al., 1994). The relative abundance of nuclear demethylated hopanes or the C₂₇ Ts/Tm ratio help identify areas where extensive paleodegradation or advanced maturity has

occurred. Two key parameters useful in distinguishing lacustrine from marine oils are compared in Figures 5 and 6. A lacustrine source is indicated when both the C₂₆:C₂₅TTP (>1.2 or even >1.5) and C₃₀:C₂₇ (>10) ratios (from m/z 259; Holba et al., 2000; 2003) are elevated and a marine source is suggested when either or both are low.

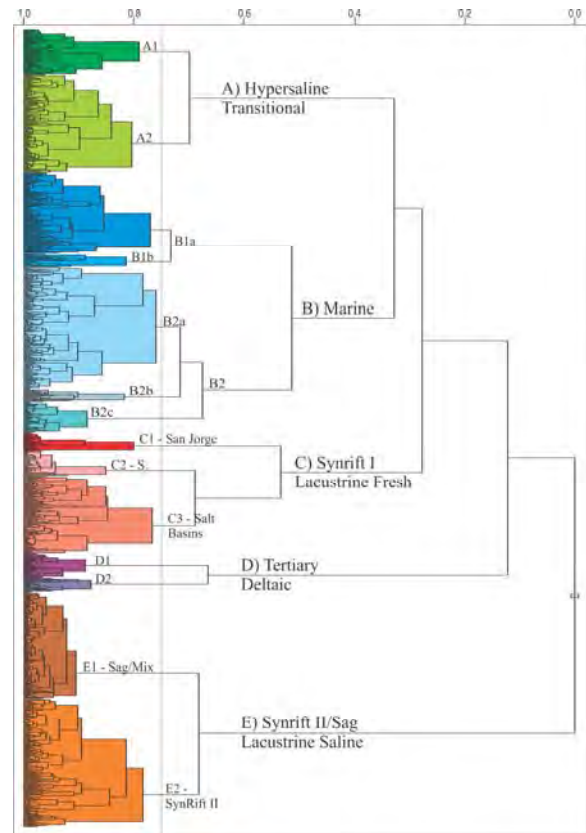


Figure 2: HCA Dendrogram for all South Atlantic Margin oils.

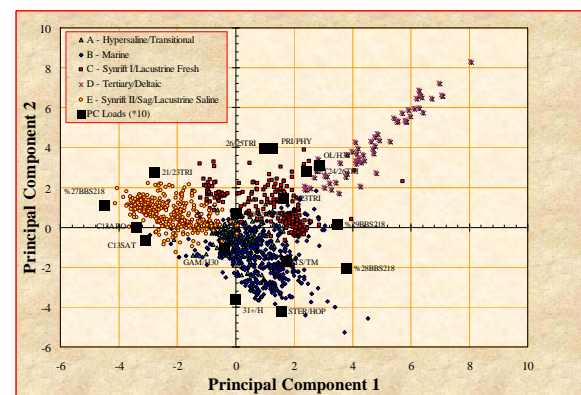


Figure 3: PCA Loads and Scores plots for all oils.

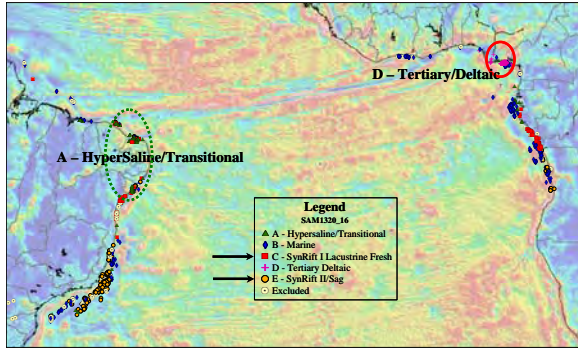


Figure 4: Distribution of South Atlantic Margin oils (Fig 2.)

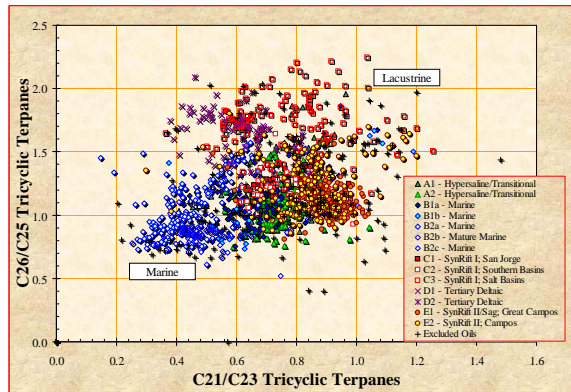


Figure 5: Tricyclic Terpene Parameters - all oils.

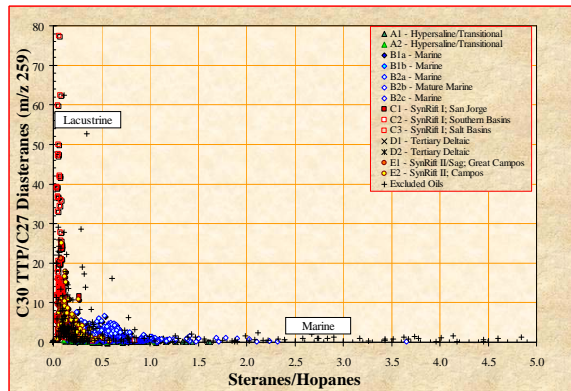


Figure 6: Sterane/Hopane ratio versus proportion of C30 Tetracyclic Terpanes (TTP) - all oils.

In order to better understand the genetic relationships established during the rifting event, a second statistical analysis was performed using only those five-hundred eighty (580) oils from families C and E thought to originate from source rocks deposited in pre-salt lacustrine environments. All marine-derived oils were excluded and

ten source dependent parameters were utilized. Two main groups of oils are distinguished; one associated with source rocks deposited in early rift environments and the second tied to Sag or Syn-Rift II depositional settings (Figures 7-9). Several sub-families exist and key parameters are compared in Figures 10-11.

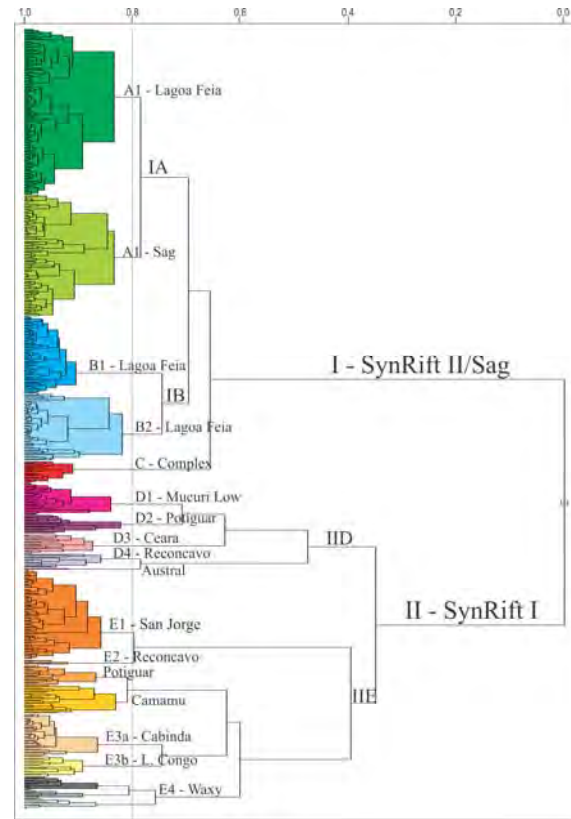


Figure 7: HCA Dendrogram for only pre-salt oils.

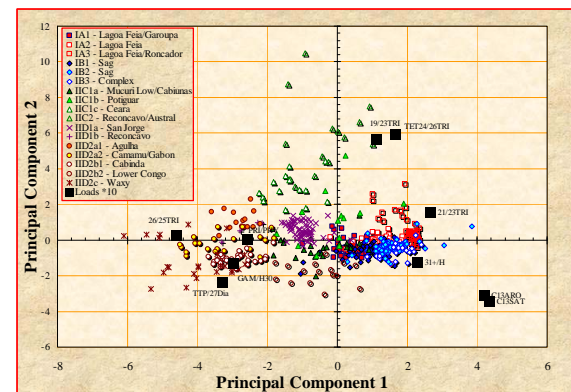


Figure 8: PCA Loads and Scores plots for pre-salt oils.

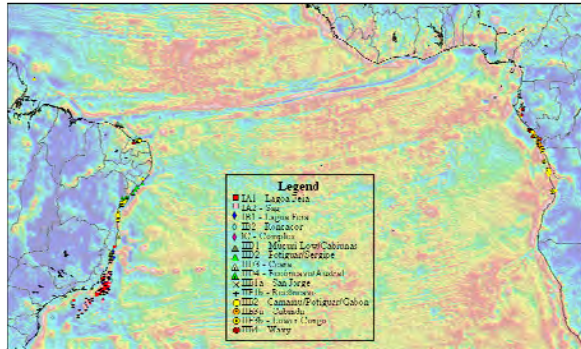


Figure 9: Distribution of South Atlantic Margin pre-salt oil families shown in Figure 7.

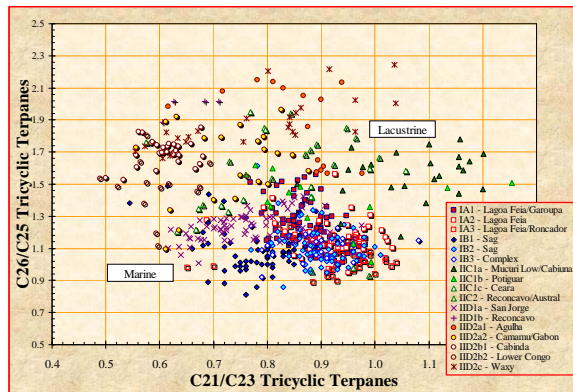


Figure 10: Tricyclic Terpene Parameters - pre-salt oils.

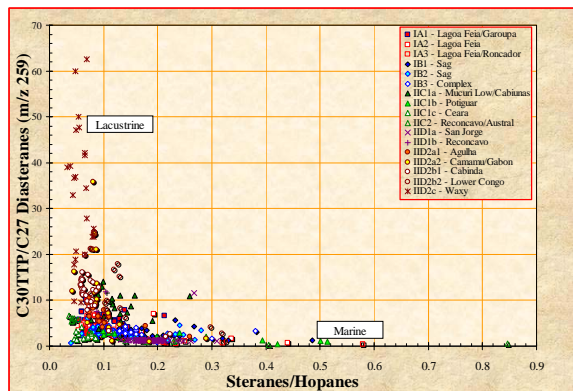


Figure 11: Sterane/Hopane vs. TTP Index - pre-salt oils.

Conclusions

The strongest genetic relationships are observed between oils from central Brazil and West Africa that originated from Barremian (Lower Rift/SynRift I) source rocks deposited in deep, freshwater lacustrine

environments. Great Campos oils appear to have a unique source chemistry. Additional samples are necessary to ensure that laboratory and sample bias are minimized.

References

Brice, S., K. Kelts, and M. Arthur, 1980. Lower Cretaceous lacustrine source beds from early rifting phases of the South Atlantic (abs.): Program with Abstracts, AAPG Annual Convention, Denver, Colorado, p. 30.

Dickson, W., C.F. Schiefelbein, C.F., M.E. Odegard and J.E. Zumberge, 2016. Petroleum Systems Asymmetry across the South Atlantic Equatorial Margins. Geological Society, London, Special Publications, 431, 3 March 2016.

Holba, A.G., Tegelaar, E., Ellis, L., Singletary, M.S., and Albrecht, P. 2000. Tetracyclic polyterpenoids: indicators of freshwater (lacustrine) algal input. *Geology* 28, p251-254.

Holba, A.G., L.I. Dzou, G.D. Wood, L. Ellis, P. Adam, P. Schaeffer, P. Albrecht, T. Greene, and W.B. Hughes, 2003. Application of tetracyclic polyprenoids as indicators of input from fresh-brackish water environments. *Org. Geochemistry* 34, no. 3: 441-469.

Mello, M.R., N.Telnaes, P.C. Gaglianone, M.I. Chicarelli, S.C. Brassell, and J.R. Maxwell, 1988. Organic geochemical characterization of depositional paleoenvironments of source rocks and oils in Brazilian marginal basins. *Organic Geochemistry*, v.13, p. 31-45.

Moldowan J.M., Fago F.J., Lee C.Y., Jacobson S.R., Watt D.S., Slougui N.E., Jeganathan A., and Young D.C., 1990. Sedimentary 24-n-propylcholestanes, molecular fossils diagnostic of marine algae. *Science* 247, 309-312.

Moldowan J.M., Dahl J., Huizinga B.J., Fago F.J., Hickey L.J., Peakman T.M., and Taylor D.W., 1994. The molecular fossil record of oleanane and its relation to angiosperms. *Science* 265, 768-771.

Schiefelbein, C.F., J.E. Zumberge, N.R. Cameron and S.W. Brown, 1999. Petroleum systems in the South Atlantic margins in Geological Society, London, Special Publication 153, p.169-179.

Schiefelbein, C.F., J.E. Zumberge, N.C. Cameron, and S.W. Brown, 2001. Geochemical comparison of crude oil, South Atlantic Margins. in: M.R. Mello & B.J. Katz (eds.), *Petroleum Systems of the South Atlantic Margin*. AAPG Memoir 73, p. 15-26.

Flexural uplift and underplating anomaly for a profile at 43.5°S on the Argentine Continental margin

Ana C. Pedraza De Marchi (1, 2), Marta E. Ghidella (3), Claudia N. Tocho (1, 4)

(1) Universidad Nacional de La Plata, Facultad de Ciencias Astronómicas y Geofísicas, La Plata, Buenos Aires, Argentina
(cpedrazadm@fcaglp.unlp.edu.ar), (2) Consejo Nacional de Investigaciones Científicas y Técnicas, Buenos Aires, Argentina, (3) Instituto Antártico Argentino, San Martín, Buenos Aires, Argentina, (4) Consejo de Investigaciones Científicas de la Provincia de Buenos Aires, Buenos Aires, Argentina.

Abstract

Magmatic underplating could be defined as “the addition of mafic magma to the lower crust and uppermost mantle around the Moho” and could be included in a wide range of processes, which appear in compressional and extensional tectonic environment as continental margins.

We have modelled the magmatic underplating effect using Process Oriented Gravity Modelling (POGM) (Watts and Fairhead, 1999) instead of conventional "static" modelling, where the density structure is determined as the best distribution that explains the observed gravity anomaly. This approach has been useful in determining the physical properties of the crust and mantle in continental margin regions. However, POGM is an innovative modelling that can distinguish the contribution that different geological processes make to the observed gravity. In the POGM the gravity anomaly is composed by the rift anomaly,

the sedimentation anomaly and the underplating anomaly.

The interest of this work is focusing in the flexural uplift produced by the magmatic underplating and its associated gravity anomaly, rarely investigated in actual profiles due to the refraction seismic data being generally unavailable. Particularly it had not been calculated in the volcanic sector of the Argentine continental margin before this work.

The obtained results give a maximum flexural uplifts associated with magmatic underplating, which are 276 m and 145 m for densities of the high-velocity body of 3050 kg/m³ and 3150 kg/m³, respectively, and an average density of the sediment of 2300 kg/m³. The increase of elastic thickness ($T_e=25\text{km}$) to a minimum *rms* in comparison with the calculation without taking into account the underplating ($T_e=20\text{ km}$) is associated with the thickening of the crust. The underplating anomaly has opposite contribution to the typical free air gravity anomaly edge-effect for the Airy and flexural case.

Introduction

Volcanic rifted margins are characterized by massive occurrences of extrusive volcanism and intrusive magmatism (magmatic underplating) formed during the rupture of the continental lithosphere and breakup (Hinz, 1981; White and McKenzie, 1989). Some authors have presented recent reviews illustrating the wide distribution of such margin that represents 75-90% of the global continental passive margins (Eldholm et al., 2000, Menzies et al., 2002). Hinz et al. (1999) showed that the relatively sparsely investigated the Argentina margin is of the volcanic type.

According to Thybo and Artemieva (2013), inside the definition of magmatic underplating are

included a wide range of processes. Underplating means “addition of mafic magma to the lower crust and uppermost mantle around the Moho” and many times has been identifying as a high-velocity body in refraction lines (Franke, 2010). Underplating takes place in a wide range of tectonic settings, and it plays a major role in the tectonomagmatic evolution of the lithosphere, for this it is impossible to provide a simple definition of the term underplating. Magmatic underplating is associated with compressional tectonic environmental (magmatic arc and crust formation, underplating of the Precambrian crust) and extensional (big extensional areas, big sills and batholiths in transition zones of the Moho, rift zones (where magma compensates the shortening of the crust and modern an paleo rift can be distinguished) and in volcanic continental margins as the volcanic sector of the Argentine continental margin (Thybo and Artemieva, 2013).

One of the most distinctive geophysical features of rifted continental margins is the free-air gravity edge-effect anomaly, which generally has been interpreted as the result of the juxtaposition of thick continental crust and thin oceanic crust.

The importance of the study of geologic, sedimentation and magmatism processes and heat diffusion phenomena that modify the initial structure of the crust for a rift and can help us to understand the distinctive characteristic of the free-air gravity edge effect of this kind of margins. A useful way to achieve this is through an oriented-processes gravity modeling (POGM) where each geologic process is associated with an anomaly. These anomalies are the rift anomaly, the sedimentation anomaly, and the magmatic underplating anomaly (Watts and Fairhead, 1999).

In simple terms, the gravity anomaly as a signature of passive margins is composed by a “high” related

with continental shelf and a “low” associated with the slope region.

In this work, the calculation of the contribution of the magmatic underplating has been taken into account in the POGM with the aim to analyze the modification that it introduces in the typical edge-effect and to calculate the flexural uplift associated. For this, we have digitized an interpreted the refraction profile by Franke et al. (2002) and Schnabel et al. (2008).

Magmatic underplating

The origin of the underplating material is unknown, but a lot of researchers have suggested (e. g. Watts, 2001), that it is generated at great depth in the mantle, which has risen due to its buoyancy (relative density differences between rising magma and surrounding rocks) and has trapped near the Moho. The magmatic underplating can cause the thickening of the crust when magma is cooled.

Xenoliths of mantle material can give us information about the last source of magma and reveal heterogeneities of magma mix and magma assimilation in deep (Beard, 2005).

The first evidence of magmatic underplating material below the continental Moho is based on the seismic and gravity data acquisition of low resolution and the results were, in general, in agreement with models of big continued layers of magmatic underplating (e.g. Fowler et al., 1989).

Recent seismic experiments (Franke et al., 2006; Franke et. al, 2010) of greater resolution have better imaged the structure of the magmatic underplating material and mafic intrusions in the continental crust and have made possible the advance in the general understanding of the processes involved (Thybo and Artemieva, 2013).

Underplating disturbs the state of isostasy of a region, so we can estimate the amount of uplift that would result by balancing a column of crust that has been underplated with one that has not (Watts, 2001).

In order to calculate the flexural effects, the appropriate wave parameter (ϕ_e) that modifies the Airy response to the one that produces the flexure is defined by $U(k) = V(k) [(\rho_a - \rho_x) / (\rho_a - \rho_w)] \phi_e(k)$, where $U(k)$ and $V(k)$ are the Fourier transform of the uplift and the thickness of the underplating, respectively, and ϕ_e is the parameter in the wave number domain.

Numerical modelling results

The modelling of the effect of the magmatic underplating has slightly increased the *rms* between the calculated with sum anomaly (Pedraza De Marchi, 2015) and the observed one, which is shown in Table 1. All models have been tested by varying the body density (ρ_x) in the range 2900 kg / m³ - 3250 kg / m³ and the density of the sediments (ρ_s) in the range 2100 kg / m³ - 2600 kg / m³. Finally, two models have been selected. Model 1 uses the density of the underplating body $\rho_x = 3050$ kg / m³; it was considered the average of the density of the crust and mantle, although we have not used a conversion law of seismic wave velocity to find the densities, standard values of crust density of 2800 kg / m³ and mantle of 3330 kg / m³ were used. Model 2 uses the parameter $\rho_x = 3150$ kg / m³ which has been interpreted by Schnabel (2008) in the same profile, we taken into account that the value that minimizes *rms* ($\rho_s = 2300$ kg / m³) is included in the range of densities 1700 kg / m³ - 2400 kg / m³ used by the author for at least two sediment layers. With the incorporation of the magmatic underplating, there is a tendency to increase the elastic thickness for the minimum *rms* because the crust became thicker with the

appearance of the magmatic underplating (Watts, 2001).

	a			b			c		
ρ_s	Te	<i>rms</i>	Te	um	<i>rms</i>	Te	um	<i>rms</i>	
2.1	25	7.5	30	251.2	8.3	30	131.6	8.1	
2.2	25	7.4	25	251.1	8.0	25	145	8.0	
2.3	20	7.3	25	276.7	7.9	25	145	7.9	
2.4	20	7.3	25	276.7	8.0	20	161.3	8.1	
2.5	20	7.6	20	307.9	8.2	20	161.3	8.2	
2.6	15	7.7	20	307.9	8.4	20	161.3	8.6	
2.7	15	7.9	15	345.2	8.7	15	180.8	8.9	

Table 1: Minimum *rms* for different densities of sedimentary thickness, a) without taking into account the underplating, b) $\rho_x = 3050$ kg / m³ and c) $\rho_x = 3150$ kg / m³. Where um is the maximum flexural uplift value.

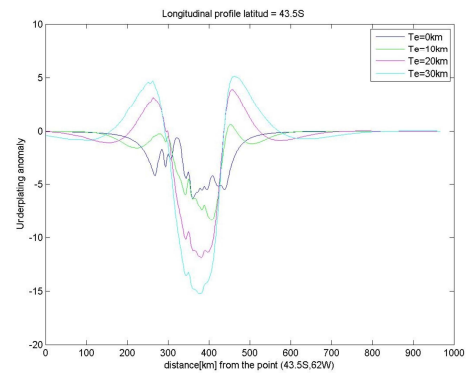


Figure 1: Underplating anomaly for different elastic thickness.

The gravity anomaly of the underplating is composed of two effects: one effect generates a low due to the low density of the underplated material and the other a high due to the displacement of the water by the uplift of the crust. This anomaly is strongly dependent on the elastic thickness (T_e) of the lithosphere, as shown in the synthetic tests by Watts et al. (1999), where for a weak margin ($T_e = 0$ km) “high” and “low” effects of the edge effect are small and with relatively long wavelength, while for a strong margin ($T_e = 20$ km) the opposite

effect occurs, the magmatic underplating increases the amplitude of the "high" and the "low" edge effect and decreases its wavelength. We have verified that the anomaly of the magmatic underplating presents opposing contributions for the cases of Airy and Flexural (Figure 1).

Conclusions

- We found a maximum flexural uplift associated with the magmatic underplating, which is 276 m ($\rho_x = 3050\text{kg/m}^3$, $\rho_s = 2300\text{kg/m}^3$) and 145 m ($\rho_x = 3150\text{kg/m}^3$, $\rho_s = 2300\text{kg/m}^3$).
- The increase of elastic thickness ($T_e=25\text{km}$) appears to be associated with the thickening of the crust, in comparison to the calculation that does not take account the magmatic underplating, that is, $T_e=20\text{km}$ according to the *rms* values.
- The underplating anomaly present opposite contributions to the Airy and flexural case as was pointed out by Watts et al. (1999) in their synthetic tests.

References

Beard, J., and C. Ragland, 2005. Reactive bulk assimilation: A model for crust-mantle mixing in silicic magmas. *Geology* 33 (8): 681–684. doi:10.1130/G21470AR.1.

Eldholm, O., T.P Gladzenko, J. Skogseid and S. Planke, 2000. Atlantic volcanic margins: a comparative study. In: Nøttvedt, A., Larsen, B.T., Olaussen, S., Tørrudbakken, B., Skogseid, J., Gabnelson, R.H., Brekke, H., Birkeland, O. (Eds.), Dynamics of the Norwegian Margin. Geological Society of London Special Publication, Vol. 167. The Geological Society, London, 411–428.

Franke, D., S. Ladage, M. Schnabel, B. Schreckenberger, C. Reichert, H. Hinz, M. Paterlini, J. de Abelleira, M. Siciliano, 2010. Birth of a volcanic margin off Argentina, South Atlantic. *Geochemistry, Geophysics, Geosystems* 11, Q0AB04.

Fowler, S.R., White, R.S., Spence, G.D., Westbrook, G.K., 1989. The Hatton Bank continental margin. 2. Deep-structure from 2-ship expanding spread seismic profiles. *Geophysical Journal of the Royal Astronomical Society* 96, 295–309.

Franke, D., Neben, S., Hinz, K., Meyer, H. and Schreckenberger, B., 2002. Hydrocarbon habitat of volcanic rifted passive margins. APG Hedberg conference.

Franke, D., Neben, S., Schreckenberger, B., Schulze, A., Stiller, M., Krawczyk, C.M., 2006. Crustal structure across the Colorado Basin, offshore Argentina. *Geophysical Journal International* 165, 850e864.

Hinz, K., 1981. A Hypothesis on Terrestrial Catastrophes. Wedges of Very Thick Oceanward Dipping Layers beneath Passive Continental Margins, *Geologische Jahrbuch*, vol. 22, Ingenta, Hannover.

Hinz, K., S. Neben, B. Schreckenberger, H. A. Roeser, M. Block, K.G.D Souza and H. Meyer, 1999. The Argentine continental margin north of 48 S: sedimentary Successions, volcanic activity during breakup. *Marine and Petroleum Geology* 16, 1e25.

Pedraza De Marchi, A. C., 2015. Caracterización isostática del sector volcánico del margen continental argentino, Tesis doctoral, Facultad de Ciencias Astronómicas y Geofísicas, Universidad Nacional de La Plata, La Plata, 174 p.

Schnabel, M., Franke, D., Engels, M., Hinz, K., Neben, S., Damm, V., Grassmann, S., Pelliza, H., Dos Santos, P.R., 2008. The structure of the lower crust at the Argentine continental margin, South Atlantic at 44S. *Tectonophysics* 454, 14e22.

Thybo, H and I. M. Almeida., 2013. Moho and magmatic underplating in continental lithosphere. *Tectonophysics*, 609, p. 605-619.

Watts, A. B. And J. D. Fairhead, 1999. A process-oriented approach to modeling the gravity signature of continental margins, *The Leading Edge*, no. 18, p. 258-263.

Watts, A. B., 2001. *Isostasy and Flexure of the Lithosphere*, Cambridge University Press.

White, R. and D. McKenzie, 1989. Magmatism at rift zones: the generation of continental margins and flood basalts. *J. Geophys. Res.* 94, 7685–7729.